

Upper-air temperature change trends above arid region of Northwest China during 1960–2009

Zhongsheng Chen · Yaning Chen · Jianhua Xu · Ling Bai

Received: 14 January 2014 / Accepted: 16 April 2014
© Springer-Verlag Wien 2014

Abstract This study summarized upper-air temperature change trends based on the monthly datasets of 14 sounding stations in the arid region of Northwest China during 1960–2009. Over the investigated period, the change in upper-air temperature measured at eight standard pressure levels shows that an obvious warming at 850–400 hPa, which decreases with altitude, changes to an apparent cooling at 300–50 hPa. There is a positive correlation between the surface and 850–300-hPa temperatures, but a negative correlation between the surface and 200–50-hPa temperatures. Over the full 1960–2009 record, patterns of statistically significant mid-lower tropospheric warming and upper tropospheric and mid-lower stratospheric cooling are clearly evident. Also, the annual temperature cycle indicates that the peak temperature shifts from July in the troposphere to February in the mid-lower stratosphere, suggesting the importance of seasonal trend analysis. We found that the warming in the mid-lower troposphere is more pronounced during the summer, autumn, and winter, whereas the cooling in the upper troposphere and mid-lower stratosphere is larger during the summer and autumn. Furthermore, there are also many regional differences in the upper-air temperature change, regardless of both season and layer.

1 Introduction

The rise in global mean surface temperatures is considered as the best-known indicator of climate change, so surface temperature change has become a topic that is increasingly popular over the recent years and receives broad media coverage (Brocard et al. 2013; IPCC 2013). However, temperature changes are not limited to the Earth's surface, but are extending to the troposphere and the stratosphere which are important components of the Earth's climate system. Changes occurring at the surface, in the troposphere, and in the stratosphere are three complementary components of climate change (Brocard et al. 2013). Moreover, the IPCC Fifth Assessment Report (IPCC 2013) also pronounced that based on multiple independent analyses of measurements from radiosondes and satellite sensors, it is virtually certain that globally the troposphere has warmed and the stratosphere has cooled since the mid-twentieth century, which suggests that global upper-air temperature variation has become an indisputable fact. As an indispensable foundation for climate-change research, the determination of the change trend of the upper-air temperature has quickly become one of the most important directions of climate-change research in recent years (Mears and Wentz 2005; Free and Seidel 2005; Herman et al. 2010; Thome et al. 2011; Seidel et al. 2011).

Due to an apparent mechanism of glaciers and snow cover melt water acceleration in response to recent climate warming in the arid region of Northwest China, the glaciers and snow cover on the high mountains have been losing mass in recent years (Kang et al. 2002; Wang et al. 2010). Obviously, it is critical to understand the climate change of the study area. Previous studies have investigated long-term surface temperature records (Shi et al. 2007; Li et al. 2012, 2013) that are easily available from weather stations in the arid region of Northwest China. The impact of upper-air warming on glaciers and snow cover on the high mountains is more important

Z. Chen · J. Xu · L. Bai
Key Laboratory of GIScience of the Ministry of Education,
East China Normal University, Shanghai 200241, China

Y. Chen (✉)
State Key Laboratory of Desert and Oasis Ecology, Xinjiang Institute
of Ecology and Geography, Chinese Academy of Sciences,
Urumqi 830011, China
e-mail: chenyn@ms.xjb.ac.cn

than that of surface warming (Zhang et al. 2010a; Chen et al. 2012). However, to date, there is still a lack of research to detect the long-term change trends of upper-air temperatures in this area. How deep in the atmosphere the current warming extends remains unclear. Furthermore, uncertain is the linkage of surface and upper-air temperatures. This study benefited from five decades of data to address these questions.

The aim of this paper is to present the radiosonde time-series data from 1960 to 2009 in the arid region of Northwest China. In this study, we checked data temporal homogeneity and then measured temporal and spatial variation of the upper-air temperatures in the troposphere and mid-lower stratosphere using the Mann-Kendall nonparametric trend test and GIS technique. Moreover, we also ascertained the extent that surface air temperature variability was linked with upper-air temperature variation and preliminarily discussed possible causes of the upper-air temperature variability.

2 Data and methods

2.1 Study area

The arid region of Northwest China refers to inland arid regions (between 73~106° E and 35~50° N) to the north of the Kunlun Mountains and the Qilian Mountains and to the west of the Helan Mountains, including the whole territory of Xinjiang Uygur Autonomous Region, the Hexi Corridor of Gansu Province, the Alashan Plateau of Inner Mongolia, and Ningxia Hui Autonomous Region to the west of Ningxia section along the Yellow River, of which the land area accounts for about one fourth of China's total area (Fig. 1). The study area, where the ecosystem is extremely weak and water resources originate mainly from the glacier melt water, snow melt water, and direct precipitation on the high mountains, is one of the most severe arid areas in the world (Shi 1995) and responds quite intensely to climate change. The glaciers and permanent snow cover on the high mountains, known as "solid reservoir," are important sources of water resources and are sensitive to changes in temperature, particularly during the spring and summer, when climate warming will promote corresponding fluctuations in glacial movement and snow distribution (Shi et al. 2007; Wang et al. 2010). At present, changes in the tropospheric temperatures have greater influences on hydrological processes by promoting the melting of glaciers and snow cover on the high mountains (Zhang et al. 2010a; Chen et al. 2012). Thus, the analysis of changes in the upper-air temperatures is particularly relevant for understanding the accelerated retreat of the glaciers and snow cover on the high mountains in the study area.

2.2 Data

Due to the lack of a dense network of sounding stations in the arid region of Northwest China, we selected only 14 sounding stations with the most continuous temperature records, and these stations can cover the entire study area. The distribution of the chosen sounding stations is shown in Fig. 1. Furthermore, owing to the limitations of radiosonde temperature records, analyses were made for only the following eight standard pressure levels in hectopascal units, i.e., 850, 700, 500, 400, 300, 200, 100, and 50.

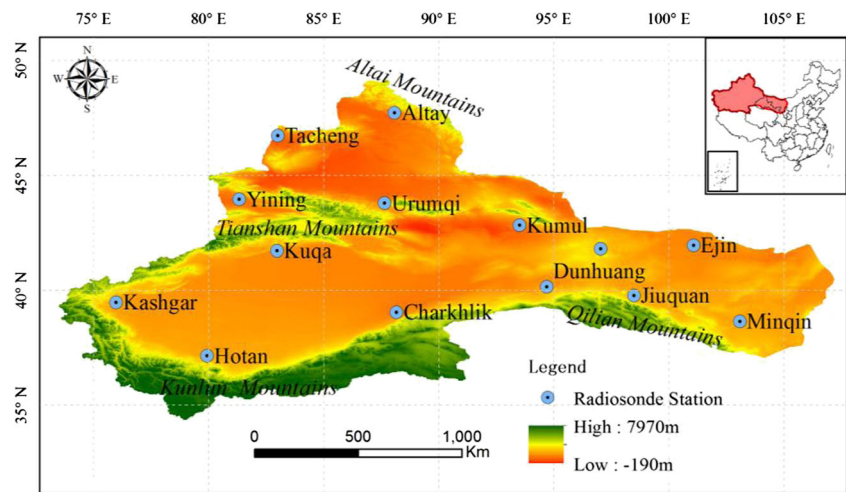
The primary data set used in this study comes from operational weather balloon soundings, that is, radiosondes, made 12-hourly during the period of 1960–2009. Data used in this study were obtained from the National Meteorological Information Center. Changing measurement practices, that is, different instruments, operational errors, and their sensitivity to environmental factors, present potential data homogeneity problems that can confound identification of climate signals (Gaffen et al. 2000; Box and Cohen 2006). To ensure data quality, the extreme decision method was used to amend the gross errors caused by operational errors in sounding observations. Moreover, the two-phase regression method was applied to homogenization on the sounding temperature's sequences with NCEP reanalysis data as reference sequences to eliminate or reduce errors of the observing system. The above revised method considers all existing historical documentation on instruments and methods used in the past and applies corrections in light of the latest knowledge. The surface air temperature used in this study is usually measured at 2 m above the ground and was obtained from the National Meteorological Information Center to compare with upper-air temperature.

2.3 Methods

Hypothesis testing for long-term trends of time series is necessary and can help discern the inherent mechanisms of a time series process. The rank-based Mann-Kendall method is a nonparametric method, commonly used to assess the significance of monotonic trends in the meteorological and hydrologic series all over the world (Douglas et al. 2000; Yue et al. 2002; Zhang et al. 2010b; Huang et al. 2013; Chen et al. 2013). In this paper, the Mann-Kendall nonparametric trend test, which is highly commended for general use by the World Meteorological Organization (Huang et al. 2013), was used to characterize the temporal trend slope as well as significant test statistics for upper-air temperature change.

The procedure of Mann-Kendall nonparametric trend test adopted in this study is as follows. In the Mann-Kendall test, there is the null hypothesis H_0 that the time series $X = \{x_1, x_2, \dots, x_n\}$, in which $n \geq 8$, is a sample of n independent and identically distributed random variables. The alternative hypothesis H_0 of a two-sided test is that the distributions of x_i and

Fig. 1 The sketch map of the arid region of Northwest China and the distribution of radiosonde stations



x_j are not identical for all i ($i=1, 2, \dots, n-1$) and j ($j=i+1, \dots, n$). The Mann-Kendall test statistic S is estimated using the following formula (Eq. 1):

$$S = \sum_{i=1}^{n-1} \sum_{j=i+1}^n \text{sgn}(x_j - x_i) \tag{1}$$

where

$$\text{sgn}(x_j - x_i) = \begin{cases} +1, & x_j > x_i \\ 0, & x_j = x_i \\ -1, & x_j < x_i \end{cases} \tag{2}$$

The statistic S is approximately normally distributed when $n \geq 8$, with the mean and the variance as formulas (Eqs. 3 and 4):

$$E(S) = 0 \tag{3}$$

$$\text{Var}(S) = \frac{n(n-1)(2n+5) - \sum_{i=1}^n t_i i(i-1)(2i+5)}{18} \tag{4}$$

where t_i is the number of ties of extent i . The standardized statistic (Z) for a one-tailed test is formulated as follows:

$$Z = \begin{cases} (S-1) / \sqrt{\text{Var}(S)}, & S > 0 \\ 0, & S = 0 \\ (S+1) / \sqrt{\text{Var}(S)}, & S < 0 \end{cases} \tag{5}$$

A positive value of Z indicates an increasing trend, and a negative value of Z indicates a decreasing trend, while a zero value of Z indicates no trend. When $|Z| > Z_{1-\alpha/2}$, in which $Z_{1-\alpha/2}$ is the standard normal deviate and α is the significance level of the test, H_0 will be rejected. At a 0.05 or 0.01 significance level, the null hypothesis of no trend is rejected if $|Z| > 1.96$ or $|Z| > 2.58$.

In the Mann-Kendall test, another very useful index is the Kendall slope, which is the magnitude of the monotonic change (Xu et al. 2003) and is given as follows:

$$\beta = \text{Median} \left(\frac{x_j - x_i}{j - i} \right), \forall j < i \tag{6}$$

where $1 < i < j < n$. The estimator β is the median overall combination of record pairs for the whole data. A positive value of β indicates an “upward trend,” whereas a negative value of β indicates a “downward trend.”

Furthermore, the correlation analysis method was used to identify a correlation between the surface temperature and upper-air temperature at each standard pressure level. The temperatures at eight standard pressure levels were compared with the surface temperature to establish the vertical profile of the correlations between the surface temperature and upper-air temperatures at eight standard pressure levels.

In this paper, we arbitrarily chose 0.05 as a reasonably high “statistical significance” threshold for the Mann-Kendall non-parametric trend test and correlation analysis method. The temperature change over the examined period is here defined as the Kendall slope β ($^{\circ}\text{C}/\text{a}$) multiplied by the time-span in years (e.g., 10 years), leaving temperature units. The aim in trend analysis is to identify significant first-order changes in mean temperature over the studied period, i.e., trends.

3 Results and discussion

3.1 Change trends of temperature at eight standard pressure levels

3.1.1 Annual change trends

Table 1 quantifies the upper-air temperature change trends during the period of 1960–2009 shown in

Fig. 2. For the period 1960–2009, 850–400-hPa warming and 300–50-hPa cooling are a dominant feature of the entire 50-year upper-air temperature record. Thereinto, 100–50-hPa cooling is more significant than 300–200-hPa cooling; warming is similar and highly significant from 850 to 400 hPa, but 500-hPa warming is the most significant. The temperature change difference at eight standard pressure levels shown in Table 1 for the period from 1960 to 2009 reaches up to 0.2 °C/10a. The upper-air temperature change in our study area is not really coherent with that of other regions (Box and Cohen 2006; Brocard et al. 2013). Over the 50 years, 850–400-hPa and surface temperatures showed similar trends in the arid region of Northwest China (not shown), which is consistent with other regions, such as Greenland (Box and Cohen 2006) and Switzerland (Brocard et al. 2013). When looking at shorter periods (not shown), it is apparent that the 50 and 300 hPa cool and the 700 hPa warms, but not evident that the 100, 200, and 400 hPa cool and the 500 and 850 hPa warm in the period 1960–1980; 850–300 hPa shows a strong warming in the period 1981–2000, followed by an insignificant warming in the period 2001–2009, and 100 and 50 hPa present a significant cooling in the period 1981–2000, followed by a slight cooling in the period 2001–2009, whereas 200 hPa presents an unimportant warming in the period 1981–2000, followed by an obvious warming in the period 2001–2009. We could conclude that except for 50 and 100 hPa, the earliest cooling period (1960–1980) appears to have dominated the long-term (1960–2009) yearly temperature decrease at 200 and 300 hPa; the warming period (1981–2000), however, has unquestionably contributed to the long-term (1960–2009) annual temperature increase from 850 to 400 hPa.

3.1.2 Correlations between upper-air temperatures and surface air temperature

To identify the linkage of upper-air temperatures and surface temperature discussed elsewhere (Li et al. 2012, 2013), we made a correlation analysis for the two. Figure 3 shows that a negative trend in the correlation between the surface and upper-air temperatures with standard pressure level decreasing is obvious. The maximum correlation is found at 850 hPa. There is a positive correlation from 850 to 300 hPa on a yearly basis, but the positive correlation remains statistically significant only up to 400 hPa. However, the correlation becomes negative at about 200 hPa upward and shows statistical significance at 50 hPa. The above asymmetry has earlier been noted (Liu and Schuurmans 1990; Wong and Wang 2000; Box and Cohen 2006). This phenomenon is linked to the heat

sources of different pressure levels. The main heat source of the troposphere is the surface longwave radiation, and the upper troposphere further away from the surface will get less heat because of energy loss in the heat-transfer process, so the temperatures in the upper troposphere are hardly dominated by the surface longwave radiation. Nevertheless, the stratosphere, far from the surface, directly receives heat from the sun's radiation, and so the temperatures at every level are not controlled by the ground longwave radiation. Therefore, we confirmed that the negative correlation between stratospheric temperature and surface temperature suggests only a statistical relationship.

3.1.3 Annual cycle

Over the course of the year, we observed seasonal variations in temperature at eight standard pressure levels. Figure 4 presents a selection of our levels illustrating the annual temperature cycle. The amplitude of the cycle is not really homogeneous at eight standard pressure levels. From 850 to 300 hPa, seasonal variation in temperature shows an evident unimodal pattern, and the peak appears in July. However, seasonal variation in temperature is a bimodal pattern at 200 and 50 hPa, and the main difference is that the peaks appear in February and July at 200 hPa, but in January and August at 50 hPa. In fact, 50 hPa can be regarded as a transition layer because of the inconspicuous seasonal variation in temperature. The seasonal variation in temperature also shows a unimodal pattern at 100 hPa, and the peak appears in February. Compared with 850–200 hPa, seasonal variation in temperature shows an opposite phase at 100 hPa, which suggests a different atmosphere structure between the troposphere and mid-lower stratosphere (Xie et al. 2013). Seasonal variation in upper-air temperature above the arid region of Northwest China is basically consistent with that of Eastern China (Xue et al. 2007; Xie et al. 2013).

3.2 Change trends of temperature in three layers

3.2.1 Annual change trends

To analyze further the change trend of upper-air temperature, we defined three layers according to previous studies on Xinjiang of Northwest China (Zhang et al. 2008) and Eastern China (Xie et al. 2013), one in the stratosphere and two in the troposphere. Figure 5 graphically displays the results for the period of 1960–2009. The lowest layer represents the mid-lower troposphere that is the average of five standard pressure levels (850, 700, 500, 400, and 300 hPa). The second layer is the upper troposphere encompassing three standard pressure levels (300, 200, and 100 hPa). The uppermost layer, namely the mid-lower stratosphere, consists of two standard pressure levels (100 and 50 hPa). The above classification results may

Table 1 Temperature trend test at eight standard pressure levels

Index	50 hPa	100 hPa	200 hPa	300 hPa	400 hPa	500 hPa	700 hPa	850 hPa
Z	-3.38 ^a	-2.02 ^a	-1.54 ^b	-1.71 ^b	3.73 ^a	4.85 ^a	4.78 ^a	4.27 ^a
Trend (°C/10a)	-0.27	-0.11	-0.08	-0.07	0.13	0.18	0.23	0.21

^a Statistically significant over the 95 % level

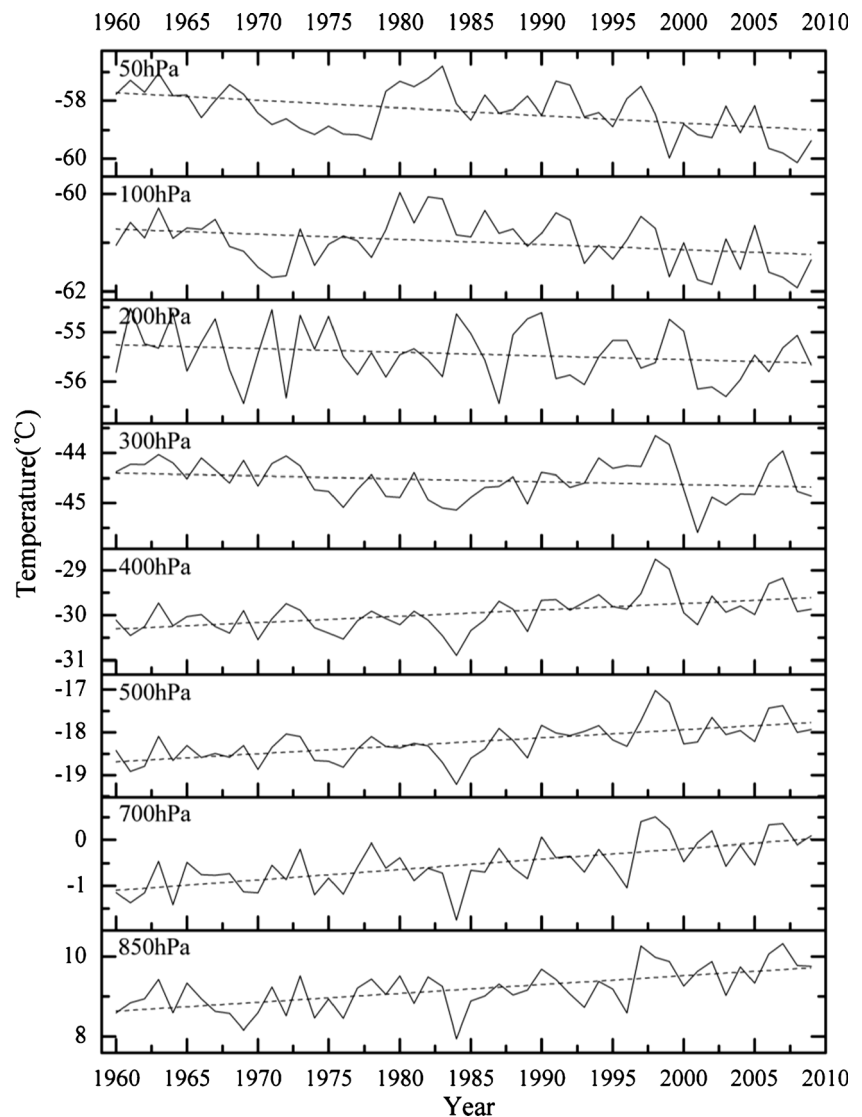
^b Statistically significant below the 95 % level

not be very accurate, but it will help us to analyze clearly the upper-air temperature change. The yearly trend in the mid-lower troposphere layer (Fig. 5) is consistent with the trend of surface temperature (not shown), as expected. The mid-lower tropospheric temperature exhibits an obvious increasing trend with a rate of +0.1 °C/10a. Above the mid-lower troposphere layer, Fig. 5 indicates a consistency in the upper troposphere and mid-lower stratosphere. The temperature trend is negative from approximately -0.1 °C/10a in the upper troposphere up

to about -0.2 °C/10a in the mid-lower stratosphere, and their decreasing trend is statistically significant, but the mid-lower stratosphere is slightly stronger than the upper troposphere.

When looking at shorter time scales (not shown), the mid-lower tropospheric temperature shows a slight decreasing trend until the early 1980s, followed by an obvious increasing trend until 2000, with a following and fairly stable situation until 2009 apart from 2006 and 2007. In the upper troposphere, we divided the time series into two subperiods as

Fig. 2 Change trends of annual temperatures at eight standard pressure levels during the period of 1960–2009. The *dashed line* means the linear trend for this period



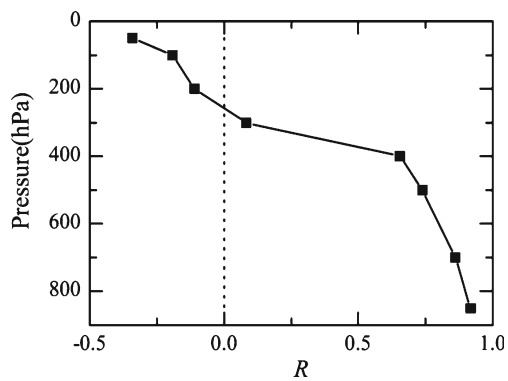


Fig. 3 Annual correlations (R) between upper-air temperatures and surface air temperature

follows: from 1960 to 2000 and from 2001 to 2009. The upper tropospheric slight cooling until 2000 is well observed, followed by an obvious warming until 2009. In the mid-lower stratosphere, we divided the time series into three sub-periods as follows: from 1960 to 1978, from 1979 to 1983, and from 1984 to 2009. The mid-lower stratospheric significant cooling until 1978 is well observed, with a cooling rate of $-0.7\text{ }^{\circ}\text{C}/10\text{a}$, followed by a short-lived warming until 1983, with an obvious cooling at a rate of $-0.5\text{ }^{\circ}\text{C}/10\text{a}$ until 2009. The above asymmetry was detected in other works, such as Cohen et al. (2012) and Brocard et al. (2013). In the mid-lower stratosphere, the period of 1979–1983 stands out as a warmer period compared to the previous and subsequent periods, but the mid-lower stratospheric cooling trend does not come to a halt. This result indicates that the mid-lower stratospheric temperature during the period of 1960–2009 has a greater period-to-period variability, implying a greater uncertainty of the mid-lower stratospheric temperature change trend.

The mechanisms of upper-air temperature change are quite a difference in the mid-lower stratosphere, upper troposphere, and mid-lower troposphere (Wang et al. 2005). In the mid-lower troposphere, the surface temperature increase can

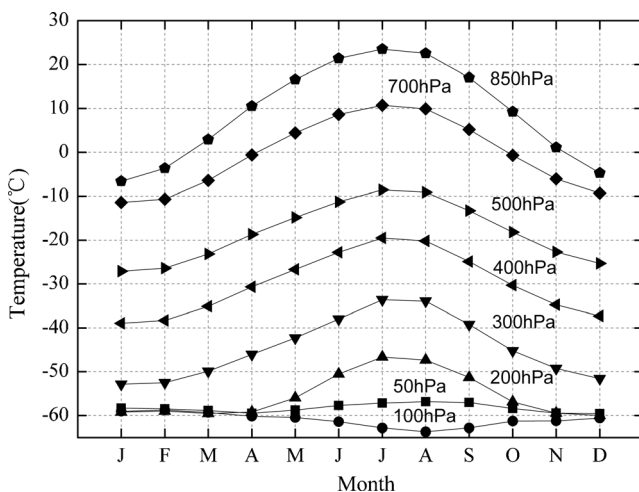


Fig. 4 Annual temperature cycle at eight standard pressure levels

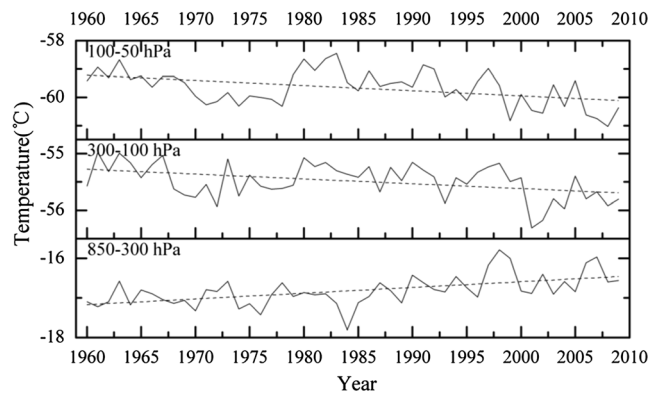


Fig. 5 Change trends of annual temperatures in three layers during the period of 1960–2009. The dashed line means the linear trend for this period

transport heat to the mid-lower troposphere by convection activities, on the one hand, and the higher content of CO_2 and water vapor, on the other hand, can absorb a large number of longwave radiations from the ground, so the surface temperature rise will inevitably lead to a temperature increase in the mid-lower troposphere. The situation, however, is different in both the upper troposphere and mid-lower stratosphere. Owing to more longwave radiation absorbed by the mid-lower troposphere, the upper troposphere will receive less longwave radiation. Meanwhile, CO_2 and water vapor increase will also transport more heat to the cosmic space in the form of infrared radiation energy. Thus, the upper tropospheric temperature will drop to some extent. In the mid-lower stratosphere, there are no convection activities because of the temperature rise with the increasing height, which means that the vertical heat transfer does not happen. The heat of the mid-lower stratosphere mainly comes from solar shortwave radiation absorbed by ozone. Generally, the ozone decreases or increases can lead to significant cooling or warming not only in the stratosphere, but also in the upper troposphere (Forster et al. 2007). In this study, we can only hope to provide a possible explanation for the mid-lower stratospheric cooling although the correlation between the mid-lower stratospheric temperature and ozone was not detected because of the lack of reliable historical ozone data.

3.2.2 Seasonal change trends

Figure 6 shows an annual temperature cycle in the mid-lower stratosphere, upper troposphere, and mid-lower troposphere. Over the course of the year, we observed large temperature variations in the troposphere. The amplitude of the cycle in the upper and mid-lower troposphere is rather homogeneous, in the order of 10 and $22\text{ }^{\circ}\text{C}$, respectively, and their peaks appear in July. Compared with the troposphere, the annual temperature cycle, however, shows a different pattern in the mid-lower stratosphere, and the peak appears in February. In the mid-lower stratosphere, the temperature in autumn is lower than

that of any other season, as seen in Fig. 6. The large yearly tropospheric temperature cycle and the special annual stratospheric temperature cycle suggest that a seasonal trend analysis is very critical. It should provide some valuable information in addition to annual trends.

Seasonal trends have been calculated (Table 2). The seasons show a year-to-year variability. However, the seasonal results also show that there are some differences from season to season, even though we have acknowledged that trend differences between some seasons are of rather low statistical significance. For instance, in the mid-lower troposphere, the trend is close to zero in spring, whereas tendencies are stronger in summer, autumn, and winter, reaching values of +0.12, +0.19, and +0.25 °C/10a, respectively. In the upper troposphere, there are considerable seasonal differences; trends are close to zero in spring and winter, but the summer and autumn trends are stronger with values reaching −0.22 and −0.10 °C/10a, respectively. In the mid-lower stratosphere, the spring trend is close to zero, and the winter trend is −0.11 °C/10a, but not a significant cooling trend compared with the summer and autumn trends with values of −0.29 and −0.27 °C/10a, respectively. The above results clearly suggest that the mid-lower stratospheric cooling is stronger in summer and autumn than in spring and winter. Similarly, the upper tropospheric cooling is lustier in summer and autumn than in spring. However, the winter has a different behavior of reversing into a nonsignificant warm trend, which suggests a larger annual temperature cycle in the upper troposphere. Conversely, the mid-lower troposphere shows a warming trend and the spring trend is similar to other seasons, although with a fewer pronounced trend. These results also point at a smaller annual temperature cycle in the mid-lower stratosphere and mid-lower troposphere compared with the upper troposphere. Perhaps our results are uncertain due to the definitions of fixed season dates and three layers, which are not necessarily representing the reality of upper-air temperature variation, but these results

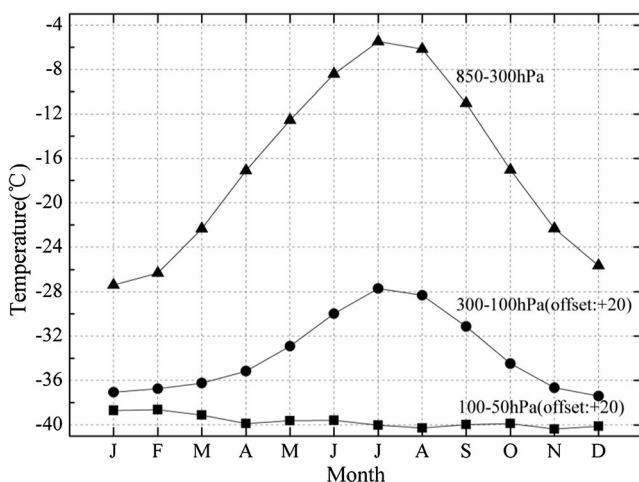


Fig. 6 Annual temperature cycle in three layers. For layers 300–100 and 100–50 hPa, a 20 °C offset is added for better visibility

Table 2 Temperature trends in three layers for different seasons

Layer	Season	Z	Trend (°C/10a)
100–50 hPa	MAM	−0.85 ^b	−0.08
	JJA	−4.07 ^a	−0.29
	SON	−4.93 ^a	−0.27
	DJF	−0.82 ^b	−0.11
300–100 hPa	MAM	−0.94 ^b	−0.05
	JJA	−5.05 ^a	−0.22
	SON	−2.93 ^a	−0.10
	DJF	0.70 ^b	0.06
850–300 hPa	MAM	0.72 ^b	0.06
	JJA	2.11 ^a	0.12
	SON	3.61 ^a	0.19
	DJF	2.91 ^a	0.25

^a Statistically significant over the 95 % level

^b Statistically significant below the 95 % level

may help us to understand deeply the condition of upper-air temperature change.

3.2.3 Distribution of change trends

Figure 7 shows that there are many regional differences in the upper-air temperature change, regardless of both season and layer. The overall average temperature in the mid-lower troposphere exhibits an increasing trend, but a decreasing trend in some regions; the upper tropospheric and mid-lower stratospheric temperatures are given priority to decline, but there are also individual regions with a rising trend. Moreover, the amplitude of temperature change is not consistent. In the mid-lower troposphere, for example, in the recent 50 years, the overall annual mean temperature presents a rising trend, but there exists a declining trend in some regions, such as the southwest of the study area; there is a stronger warming trend in the northern Xinjiang and Hexi Corridor. In the spring, the temperature shows an overall weak upward trend, except for three regions that have a significant rising trend, whereas the temperature is given priority to falling in the southern Xinjiang, where the temperature shows an obvious drop trend in Hotan. In the summer, the temperature presents a dramatic rising trend; the notable upward trend appears primarily in Altay, Tacheng, Tianshan Mountains, and west-middle section of the Qilian Mountains; the cooling trend is mainly concentrated in the southwest of the study area. In the autumn, the temperature shows an obvious increasing trend; the pronounced warming trend is mainly concentrated in the northern Xinjiang, west-middle section of the Qilian Mountains. Meanwhile, Hotan shows a weak downward trend. In the winter, all regions show a warming trend, and among them, there is a significant increasing trend in the Altay, Tianshan Mountains, and Hexi Corridor.

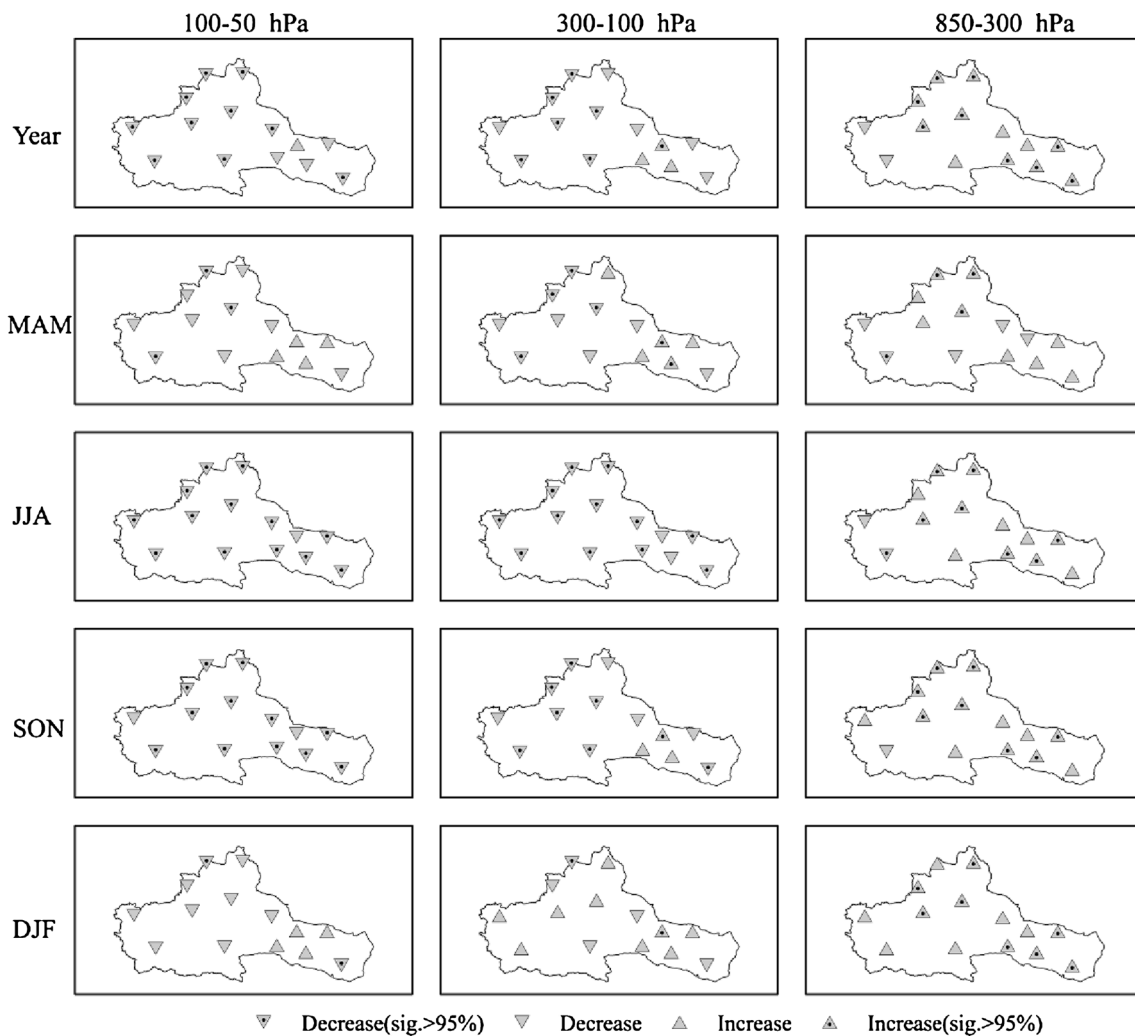


Fig. 7 Distribution of the trend changes in the upper-air temperature in three layers on different time scales

There are many factors that affect the above regional differences in upper-air temperature change. Firstly, since the upper-air temperature change can reflect the circulation variations of the cold air mass and warm air mass in the high atmosphere, the unique circulation characteristics in different regions are also bound to affect greatly the changes in the upper-air temperature. Secondly, elevation is an indispensable factor, and different elevation locations correspond to different change degrees in the upper-air temperature change. Thirdly, the underlying surface also has a certain impact on changes in the upper-air temperature by affecting longwave radiation from the surface to upper-air. Additionally, the types and intensity of human activities are different in each area; meanwhile, land use/cover is also different, so greenhouse gases and aerosols from human activities will contribute to the individual upper-air temperature change in the locality. We also noted that southwest of the study area, especially in Hotan, the upper-air temperature change showed a unique regional feature. The southwest of the study area is located in the northwestern edge of the Qinghai-Tibet Plateau, where

the upper-air temperature change may be related to changes in thermal effects of the Qinghai-Tibet Plateau. Ye et al. (1957) and Flohn (1957) found that the Qinghai-Tibet Plateau not only played a dynamic role in forcing large-scale air flow around or climbing with its huge mountains, but also was the heat source uplifted to the middle layer of the troposphere to heat directly the atmosphere there. With thermic effects to change the upper atmospheric thermal conditions, the Qinghai-Tibet Plateau can affect the atmospheric circulation and climate in the surrounding and adjacent areas.

4 Conclusions

This paper shows a summary of 50 years of radiosonde temperature measurements at the 14 sounding stations in the arid region of Northwest China. The data set used is the result of a high-quality revision of the original radiosonde data. The revised method considers all existing historical documentation

on instruments and methods used in the past and applies corrections in light of the latest knowledge.

Temperature trends measured at eight standard pressure levels over the investigated period are not entirely consistent with the trends shown in the existing literature. An obvious warming at 850–400 hPa, which decreases with altitude, changes to a clear cooling at 300–50 hPa during the period 1960–2009. Thereinto, 100–50 hPa cooling is more significant than 300–200 hPa cooling, and 500 hPa warming is the most remarkable. It is clear that the earliest cooling period (1960–1980) has dominated the long-term (1960–2009) annual temperature decrease at 200 and 300 hPa, whereas the warming period (1981–2000) has unquestionably contributed to the long-term (1960–2009) yearly temperature increase from 850 to 400 hPa. Meanwhile, the asymmetry is also clearly evident in the vertical profile of correlation between surface and upper-air annual temperature variability.

The three layers were defined according to previous studies, namely mid-lower troposphere, upper troposphere, and mid-lower stratosphere. Systematic patterns of tropospheric and mid-lower stratospheric temperature change above the arid region of Northwest China were evident in radiosonde data spanning the 1950–2009 period. The current 50-year period is marked by statistically significant mid-lower tropospheric warming and upper tropospheric and mid-lower stratospheric cooling. It is clearly evident in the asymmetry between mid-lower tropospheric and upper tropospheric, mid-lower stratospheric temperature variability. The large annual tropospheric temperature cycle and the special annual stratospheric temperature cycle suggest that a seasonal trend analysis is very important. We concluded that the warming in the mid-lower troposphere is more pronounced during the summer, autumn, and winter, whereas the cooling in the upper troposphere and mid-lower stratosphere is greater during the summer and autumn. Furthermore, the upper tropospheric temperature has a different behavior of reversing into a non-significant warm trend in winter. Due to numerous existing influencing factors, such as local topography, atmospheric circulation, and human activities, there are many regional differences in the upper-air temperature change, regardless of both season and layer.

The current study reveals that the variations of annual and seasonal temperatures in the mid-lower troposphere and in the upper troposphere, mid-lower stratosphere are very different and often opposite, which suggests that temperature changes in the three layers are disconnected and driven by different physical phenomena. However, the physical phenomena affecting upper-air temperature change were not discussed in an in depth manner in this paper and need further dissecting in a future study.

Acknowledgments The research was supported by the National Basic Research Program of China (973 Program, no. 2010CB951003) and the

Postgraduate Scholarships for Academic Innovation of East China Normal University.

References

- Box JE, Cohen AE (2006) Upper-air temperatures around Greenland: 1964–2005. *Geophys Res Lett* 33(12), L12706. doi:10.1029/2006GL025723
- Brocard E, Jeannot P, Begert M, Levrat G, Philipona R, Romanens G, Scherrer SC (2013) Upper air temperature trends above Switzerland 1959–2011. *J Geophys Res* 118(10):4303–4317
- Chen ZS, Chen YN, Li WH (2012) Response of runoff to change of atmospheric 0°C level height in summer in arid region of Northwest China. *Sci China Earth Sci* 55(9):1533–1544
- Chen ZS, Chen YN, Li BF (2013) Quantifying the effects of climate variability and human activities on runoff for Kaidu River Basin in arid region of northwest China. *Theor Appl Climatol* 111(3–4):537–545
- Cohen JL, Furtado JC, Barlow M, Alexeev VA, Cherry JE (2012) Asymmetric seasonal temperature trends. *Geophys Res Lett* 39(4), L04705. doi:10.1029/2011GL050582
- Douglas EM, Vogel RM, Kroll CN (2000) Trends in floods and low flows in the United States: impact of spatial correlation. *J Hydrol* 240(1–2):90–105
- Flohn H (1957) Large-scale aspects of the “summer monsoon” in south and East Asia. *J Meteor Soc Jpn* 75:180–186
- Forster PM, Bodeker G, Schofield R, Solomon S, Thompson D (2007) Effects of ozone cooling in the tropical lower stratosphere and upper troposphere. *Geophys Res Lett* 34(23), L23813. doi:10.1029/2007GL031994
- Free M, Seidel DJ (2005) Causes of differing temperature trends in radiosonde upper air data sets. *J Geophys Res* 110(D7), D07101. doi:10.1029/2004JD005481
- Gaffen DJ, Sargent MA, Habermann RE, Lanzante JR (2000) Sensitivity of tropospheric and stratospheric temperature trends to radiosonde data quality. *J Clim* 13(10):1776–1796
- Herman BM, Brunke MA, Pielke RA, Christy JR, McNider RT (2010) Satellite global and hemispheric lower tropospheric temperature annual temperature cycle. *Remote Sens Environ* 2(11):2561–2570
- Huang J, Sun SL, Zhang JC (2013) Detection of trends in precipitation during 1960–2008 in Jiangxi province, southeast China. *Theor Appl Climatol* 114(1–2):237–251
- IPCC (2013) *Climate change 2013: the physical science basis*. Cambridge Univ Press, UK
- Kang ES, Cheng GD, Dong ZC (2002) *Glacier-snow water resources and mountain runoff in the arid area of Northwest China*. Science Press, Beijing, In Chinese
- Li BF, Chen YN, Chen ZS, Li WH (2012) Trends in runoff versus climate change in typical rivers in the arid region of northwest China. *Quatern Int* 282:87–95
- Li BF, Chen YN, Shi X, Chen ZS, Li WH (2013) Temperature and precipitation changes in the diverse environments in the arid region of northwest China. *Theor Appl Climatol* 112(3–4):589–596
- Liu Q, Schuurmans CJE (1990) The correlation of tropospheric and stratospheric temperatures and its effect on the detection of climate changes. *Geophys Res Lett* 17(8):1085–1088
- Mears CA, Wentz FJ (2005) The effect of diurnal correction on satellite-derived lower tropospheric temperature. *Science* 309: 1548–1551
- Seidel DJ, Gillett NP, Lanzante JR, Shine KP, Thorne PW (2011) Stratospheric temperature trends: our evolving understanding. *WIREs: Clim Chang* 2(4):592–616

- Shi YF (1995) The impact of water resources under climate change in Northwest and North China. Shandong Science and Technology Press, Ji'nan, In Chinese
- Shi YF, Shen YP, Kang ES, Li DL, Ding YJ, Zhang GW, Hu RJ (2007) Recent and future climate change in Northwest China. *Clim Chang* 80(3–4):379–393
- Thorne PW, Lanzante JR, Petersom TC, Seidel DJ, Shine KP (2011) Tropospheric temperature trends: history of an ongoing controversy. *WIREs: Clim Chang* 2(1):66–88
- Wang SW, Zhao ZC, Gong DY (2005) Introduction to modern climatology. China Meteorological Press, Beijing
- Wang J, Li HY, Hao XH (2010) Responses of snowmelt runoff to climatic change in an inland river basin, Northwestern China, over the past 50 years. *Hydrol Earth Syst Sci* 14(10):1979–1987
- Wong S, Wang WC (2000) Interhemispheric asymmetry in the seasonal variation of the zonal mean tropopause. *J Geophys Res* 105(D21):26645–26660
- Xie X, Qi L, He JH (2013) An analysis on upper-air temperature over Eastern China during 1980–2009. *Adv Clim Chang Res* 9(2):102–109, In Chinese
- Xu ZX, Takeuchi K, Ishidaira H (2003) Monotonic trend and step changes in Japanese precipitation. *J Hydrol* 279(2–3):144–150
- Xue DQ, Tan ZM, Gong DL, Wang XT (2007) Primary analyses of upper-air temperature changes in China in past 40 years. *Plateau Meteor* 26(1):141–149, In Chinese
- Ye DZ, Luo SW, Zhu BZ (1957) The wind structure and heat balance in the lower troposphere over Tibetan Plateau and its surroundings. *Acta Meteorol Sin* 28:108–121, In Chinese
- Yue S, Pilon P, Cavadias G (2002) Power of the Mann-Kendall and Spearman's rho tests for detecting monotonic trends in hydrological series. *J Hydrol* 259(1–4):254–271
- Zhang GX, Zhao L, Sun SF (2008) Analysis of some facts and abrupt change of upper air temperature in Xinjiang during 1961–2000. *J Desert Res* 28(5):908–914, In Chinese
- Zhang GX, Sun SF, Ma YF, Zhao L (2010a) The response of annual runoff to the height change of the summertime 0°C level over Xinjiang. *J Geogr Sci* 20(6):833–847
- Zhang Q, Xu CY, Zhang ZX, Chen X, Han ZQ (2010b) Precipitation extremes in a karst region: a case study in the Guizhou province, southwest China. *Theor Appl Clim* 101(1–2):53–65